Biophysical Chemistry, 33 (1989) 77–90
Elsevier

BPC 01345

Simultaneous analysis of single-photon timing data for the one-step determination of activation energies, frequency factors and quenching rate constants

Application to tryptophan photophysics

Noël Boens, Luc D. Janssens and Frans C. De Schryver

Department of Chemistry, Katholieke Universiteit Leuven, B-3030 Heverlee, Belgium

Received 11 July 1988
Revised manuscript received 25 November 1988
Accepted 12 December 1988

Single-photon timing; Activation energy; Fluorescence decay; Tryptophan; Global analysis; Quenching rate constant

A general global analysis of single-photon timing data is presented in which each fluorescence decay curve can be described by a different decay law. The model parameters can be held in common within one curve and/or between related curves. Any or all parameters can be kept fixed, or they may be variable to seek optimum values. This general analysis allows the determination of activation energies, frequency factors and quenching rate constants in one step. The construction of the global mapping table which relates parameters in one experiment to those in another is explained in detail. The use and performance of this general simultaneous analysis are examined using tryptophan fluorescence decays at pH 6.0 obtained at various emission wavelengths as a function of temperature and added solute quencher. The results show that tryptophan at pH 6.0 decays as a biexponential with decay times which are independent of the analysis wavelength. The decay component with the short lifetime has a deactivation rate constant of 1.4×10^{9} s^{-1} independent of temperature. The decay component with the long lifetime has an activation energy of 28 kJ/mol and a frequency factor of 3×10^{13} s^{-1}; its temperature-independent decay rate constant equals 1×10^{8} s^{-1}. Recursion formulas for a computer program to estimate activation energies, frequency factors, and decay rate constants are provided.

1. Introduction

Time-resolved fluorescence measurements [1–3] are a valuable tool in our understanding of the often complex photophysical behavior of biological systems. In order to identify the model for an intricate physical system, time-resolved fluorescence experiments are performed under different conditions of pH, temperature, quenching, etc. In the conventional (single-curve) data analysis, the fluorescence decays are described individually by mathematical equations, and a proposed model is tested by the consistency of the recovered parameters. A subsequent analysis of the parameter estimates provides the parameters of interest. In most cases, exponential decay times τ_i and their associated scaling factors α_i are used to describe the physical system. This analysis approach, though adequate in many cases, fails to take full advantage of relations that may exist between individual decays. The simultaneous (global) analysis [4–7] of multiple decays utilizes (and tests) those relationships by keeping some model parameters in common between different related experiments. This type of analysis imposes the model directly on the actual decay data. The advantages

Correspondence address: N. Boens, Department of Chemistry, Katholieke Universiteit Leuven, B-3030 Heverlee, Belgium.

of the global analysis method are the improved model testing capability and accuracy of the recovered parameters in comparison to single-curve analysis. In the global analysis, the parameters held common between similar decays can be the decay times τ_i. However, in most instances, τ_i values will vary between related experiments. The set of α_i, τ_i values are thus empirical descriptors of the fluorescence decays. The primary parameters of interest in simultaneous analysis are decay rate constants, frequency factor, activation energy, enthalpy and entropy.

The time-resolved fluorescence of tryptophan continues to be the focus of many investigations. The effects of temperature, quencher concentration, pH and emission wavelength have been studied using single-curve analysis. Good fits to the decay data were obtained by an analysis in terms of discrete α_i and τ_i. These results, however, did not elucidate the puzzle of tryptophan photophysics.

Therefore, in order to clarify the photophysics of tryptophan we measured fluorescence decays of tryptophan at pH 6.0 at multiple temperatures, quencher concentrations and emission wavelengths. The fluorescence decay data surfaces were subsequently simultaneously analyzed in terms of various discrete decay rate constants, activation energies and prefactors. This global analysis of the entire fluorescence decay surface is well-suited for investigating the complex photophysical behavior of tryptophan.

2. Experimental

2.1. Chemicals

p-Terphenyl (Merck, scintillation grade) and 1,4-bis(4-methyl-5-phenyloxazol-2-yl)benzene (dimethyl-POPOP, Kodak, scintillation grade) were used as received. Xanthione was synthesized and purified as described earlier [8]. L-Tryptophan (Sigma) was recrystallized from water/ethanol. Na_2HPO_4, NaH_2PO_4 (both from Janssen, ACS reagent) and acrylamide (Bio-Rad Laboratories, electrophoresis purity reagent) were used without further purification. All fluorescence decay measurements were carried out in Na_2HPO_4-NaH_2PO_4 buffer solution at pH 6.0 [9]. The temperature of the solutions was kept constant to within $\pm 0.2°C$. Deionized, double-distilled water was used to prepare the buffer solutions.

2.2. Instrumentation

Fluorescence decay curves were obtained using the 295 nm excitation of a Spectra-Physics frequency-doubled, mode-locked, cavity-dumped, synchronously pumped R6G dye laser with single-photon timing detection [1–3]. All fluorescence decay curves were collected in $\frac{1}{2}$K data points of the multichannel analyzer and contained between 6×10^3 and 10^4 peak counts. All samples were deoxygenated by bubbling argon gas through the solutions before measurement. Details of the fluorescence lifetime apparatus and the associated optical and electronic components are described elsewhere [10].

2.3. Reference convolution in the analysis of single-photon timing data

In an ideal single-photon timing experiment, the time-resolved fluorescence profile of the sample, $d_s(t,\lambda_{ex},\lambda_{em})$, obtained by excitation at wavelength λ_{ex} and observed at emission wavelength λ_{em}, can be written as

$$d_s(t,\lambda_{ex},\lambda_{em}) = \int_0^t u(t-s,\lambda_{ex},\lambda_{em}) f_s(s,\lambda_{ex},\lambda_{em})\, ds \qquad (1)$$

where $u(t,\lambda_{ex},\lambda_{em})$ denotes the instrument response function and $f_s(t,\lambda_{ex},\lambda_{em})$ the δ-response of the sample. We used the reference convolution method [11–16] to correct for the wavelength dependence of $u(t)$.

In this method the decay of a reference compound, $d_r(t,\lambda_{ex},\lambda_{em})$, is measured at the same instrumental settings as used for the sample. The parameters of the modified sample response function $\tilde{f}_s(t)$ which satisfies the equation

$$d_s(t,\lambda_{ex},\lambda_{em}) = \int_0^t d_r(t-s,\lambda_{ex},\lambda_{em}) \tilde{f}_s(s,\lambda_{ex},\lambda_{em})\, ds \qquad (2)$$

are obtained from the measured decay profiles $d_s(t)$ and $d_r(t)$ using a standard deconvolution method [17–19]. It has been shown [11–16] that, if the reference compound decays with single-exponential kinetics,

$$f_r(t) = a_r \exp(-t/\tau_r) \tag{3}$$

where τ_r denotes the decay time of the reference material and a_r its corresponding scaling factor, $\tilde{f}_s(t)$ that satisfies eq. 2 is given by

$$\tilde{f}_s(t) = a_r^{-1}\left[f_s(0)\delta(t) + f_s'(t) + f_s(t)/\tau_r\right] \tag{4}$$

where $\delta(t)$ is the Dirac delta function and $f_s'(t)$ denotes the time derivative. In this paper, we shall consider quenching (eqs. 5 and 6) and the temperature dependence (eqs. 7 and 8) of fluorescence.

$$f_s(t) = \sum_{m=1}^{p} a_s^m \exp\left[-t\left(k_{oq}^m + k_q^m[Q]\right)\right] \tag{5}$$

$$\tilde{f}_s(t) = \sum_{m=1}^{p} \alpha^m \delta(t) + \sum_{m=1}^{p} \alpha^m \left(1/\tau_r - k_{oq}^m - k_q^m[Q]\right) \times \exp\left[-t\left(k_{oq}^m + k_q^m[Q]\right)\right] \tag{6}$$

$$f_s(t) = \sum_{m=1}^{p} a_s^m \times \exp\left\{-t\left[k_{ot}^m + A^m \exp(-E_a^m/RT)\right]\right\} \tag{7}$$

$$\tilde{f}_s(t) = \sum_{m=1}^{p} \alpha^m \delta(t) + \sum_{m=1}^{p} \alpha^m \left[1/\tau_r - k_{ot}^m - A^m \times \exp(-E_a^m/RT)\right] \times \exp\left\{-t\left[k_{ot}^m + A^m \exp(-E_a^m/RT)\right]\right\} \tag{8}$$

p denotes the number of exponential terms considered in the decay, a_s^m and α^m ($\alpha^m = a_s^m/a_r$) are preexponentials. τ_r denotes the reference lifetime. In eqs. 5 and 6, k_{oq}^m and k_q^m represent the decay rate constant in the absence of quencher Q and the bimolecular quenching rate constant for the m-th exponential term, respectively. In eqs. 7 and 8, k_{ot}^m, E_a^m and A^m are, respectively, the temperature-independent decay rate constant, activation energy and frequency factor for the m-th exponential. In the appendix, recursion formulas are given which reduce the computation time considerably.

2.4. Global data analysis

In single-photon timing experiments the nonlinear mathematical model is of the form $y = f(t,\boldsymbol{\theta})$ where t (time) and y (decay data) are observable variables and $\boldsymbol{\theta}$ the unknown parameter vector with p components. In nonlinear least-squares algorithms based upon expanding y^c (the fitted decay data) in a first-order Taylor series, the $p \times 1$ column vector $\boldsymbol{\delta}$ of the incremental change in the parameter vector $\boldsymbol{\theta}$ is the solution of eq. 9:

$$\boldsymbol{A}\boldsymbol{\delta} = \boldsymbol{g} \tag{9}$$

$\boldsymbol{A}$ is a $p \times p$ matrix, $\boldsymbol{g}$ and $\boldsymbol{\delta}$ being $p \times 1$ column vectors with elements

$$A_{jk} = \sum_{i=1}^{n} w_i \frac{\partial y_i^c}{\partial \theta_j} \frac{\partial y_i^c}{\partial \theta_k} \tag{10a}$$

$$g_k = \sum_{i=1}^{n} w_i \frac{\partial y_i^c}{\partial \theta_k}(y_i - y_i^c) \tag{10b}$$

$$\delta_k = \text{incremental change in parameter } \theta_k \tag{10c}$$

In the single-curve analysis approach, the matrices $\boldsymbol{A}$ and $\boldsymbol{g}$ with elements defined in eq. 10 are constructed and eq. 9 is solved for each individual decay curve. In the global analysis, however, the matrices for the individual experiments are not constructed because information from similar experiments determines the fitting parameter estimates. The global equation corresponding to eq. 9 is given by

$$\boldsymbol{A}^G\boldsymbol{\delta}^G = \boldsymbol{g}^G \tag{11}$$

where the superscript G denotes global, $\boldsymbol{A}^G$ is a $q \times q$ matrix, $\boldsymbol{g}^G$ and $\boldsymbol{\delta}^G$ are $q \times 1$ column vectors with q the number of independent (global) fitting parameters (free and fixed) of the analysis. The matrices $\boldsymbol{A}^G$, $\boldsymbol{g}^G$ and $\boldsymbol{\delta}^G$ have elements

$$A_{jk}^G = \sum_{l=1}^{r} \sum_{i=1}^{n} w_{li} \frac{\partial y_{li}^c}{\partial \theta_j^G} \frac{\partial y_{li}^c}{\partial \theta_k^G} \tag{12a}$$

$$g_k^G = \sum_{l=1}^{r} \sum_{i=1}^{n} w_{li} \frac{\partial y_{li}^c}{\partial \theta_k^G}(y_{li} - y_{li}^c) \tag{12b}$$

$$\delta_k^G = \text{incremental change in parameter } \theta_k^G \tag{12c}$$

Eqs. 11 and 12 are formally equivalent to eqs. 9 and 10, respectively. The summation, however, is over the entire decay surface (consisting of r experiments). In the simultaneous analysis, parameters which are in common between different decay experiments will give rise to matrix elements of $\boldsymbol{A}$ and $\boldsymbol{g}$ that can be summed together in the respective global matrices $\boldsymbol{A}^{\mathrm{G}}$ and $\boldsymbol{g}^{\mathrm{G}}$. Therefore, a general method for mapping the local matrices $\boldsymbol{A}$ and $\boldsymbol{g}$ into the global matrices $\boldsymbol{A}^{\mathrm{G}}$ and $\boldsymbol{g}^{\mathrm{G}}$ is required. This mapping scheme must not be bound to any model. Brand and co-workers [5,7] proposed the construction of a global mapping matrix containing the independent global parameter indices to relate parameters in one experiment to those in another. We extend their idea to a general global mapping table **M** allowing different decay laws to be combined in one global analysis. The global mapping table **M** can be created and modified using a full-screen editor (e.g., EDIT (MS-DOS) for IBM (compatible) PCs or INed for IBM RT PC). An example of a global mapping table is given in table 1A. The row index corresponds to the experiment (curve) number included in the global analysis. $M(i,0)$ is the function selection number defining the model to be fitted to the experimental data of the i-th decay. The elements $M(i,j)$ $(j=1,\ldots,p)$ are the global parameter indices. The numbers 0 or 1 after the parameter index and separated by a vertical bar indicate whether the value of that parameter is to be kept constant (1) or not (0) during the fitting. Only 0 and 1 are acceptable for that purpose. Any or all model parameters can be held fixed, or they may vary to seek optimum values. Parameters are held in common within one curve and/or between related curves when they appear more than once in the global mapping table. Evidently, a linked parameter cannot be constant and variable at the same time. After creation/modification, the contents of the global mapping table are examined to ensure that all information is valid and compati-

Table 1

Global mapping table (A) for a global analysis with four experiments and four different decay laws

The estimated parameters from global (B) and individual analyses (C) are given. Numbers between parentheses in part C are global parameter indices. See text for more details.

(A)	1	1|0	2|0	3|1		
	2	4|0	2|0	5|0	6|0	3|1
	6	7|0	6|0	8|0	9|0	3|1
	37	10|0	11|0	12|0	9|0	

Parameter index		True value	Fitted value (±S.D.)
(B)	1	0.571	0.572 ± 0.001
	2	100 ns	99.92 ± 0.11
	3	5 ns	5 (held fixed)
	4	0.119	0.122 ± 0.003
	5	0.405	0.399 ± 0.002
	6	200 ns	200.57 ± 0.51
	7	0.524	0.524 ± 0.001
	8	0.1	0.104 ± 0.005
	9	$1\times10^{7}\ s^{-1}$	$9.89 \pm 0.27\times10^{6}$
	10	0.230	0.230 ± 0.001
	11	$5\times10^{6}\ s^{-1}$	$4.94 \pm 0.04\times10^{6}$
	12	1000 M^{-1}	1026.3 ± 21.5

(C)	Curve 1	0.572 ± 0.001 (1)	99.93 ± 0.11 (2)	5 (held fixed) (3)	
	Curve 2	0.106 ± 0.025 (4)	93.72 ± 10.98 (2)	0.415 ± 0.026 (5)	198.00 ± 4.27 (6)
	Curve 3	0.523 ± 0.001 (7)	202.22 ± 2.01 (6)	0.120 ± 0.021 (8)	$8.08 \pm 1.70\times10^{6}$ (9)
	Curve 4	0.230 ± 0.001 (10)	$4.95 \pm 0.04\times10^{6}$ (11)	1022.9 ± 20.7 (12)	$9.94 \pm 0.26\times10^{6}$ (9)

ble. The correctness of the function selection number is checked, the corresponding number of model parameters calculated, and the presence of the needed parameter indices investigated. The number of global parameters q is determined and the global mapping table is inspected to verify that all parameter indices from 1 to q are present. The frequency of each parameter index is counted. When more than one curve is analyzed, at least one linked parameter per experiment is needed. However, the program, based on Marquardt's algorithm [20], can perform single-curve analysis. The entire decay profile, including the rising edge, was analyzed. In this procedure, several fluorescence decays at different quencher concentrations [Q] were analyzed simultaneously according to eq. 1 with $f_s(t)$ given by eq. 5 or according to eq. 2 with $\tilde{f}_s(t)$ described by eq. 6. The model parameters k_{oq}^m and k_q^m were linked between all the experiments. Multiple fluorescence decays at various temperatures (between 20 and 60 °C) were analyzed simultaneously according to eq. 1 with $f_s(t)$ given by eq. 7 or according to eq. 2 with $\tilde{f}_s(t)$ described by eq. 8. The model parameters k_{ot}^m, E_a^m and A^m were held in common. More complex linking schemes were also applied (e.g., see table 2). In most analyses, the reference lifetime τ_r was kept fixed at its known value (1.04 ns for *p*-terphenyl in isooctane, 1.24 ns for dimethyl-POPOP in isooctane, 45 ps for xanthione in isooctane). Standard deviations of the parameters were calculated from the parameter covariance matrix. In the single-curve analyses the decay times τ_i and corresponding scaling factors α_i were estimated. Values of k_{oq}^m and k_q^m were obtained from a linear regression of τ_m^{-1} vs. [Q]. Values of k_{ot}^m, E_a^m and A^m were calculated by a nonlinear least-squares analysis of τ_m as a function of temperature.

The statistical criteria used to assess the goodness-of-fit in the simultaneous analysis of fluorescence decay surfaces include plots of autocorrelation function values [21] vs. experiment number, and of weighted residuals vs. channel number vs. experiment number. The numerical statistical tests are the calculation of the global reduced chi-square statistic χ_g^2 and its normal deviate $Z_{\chi_g^2}$. Fits with $|Z_{\chi_g^2}| < 3$ were considered acceptable. The goodness-of-fit of the individual decay curves was examined by the Durbin-Watson test statistic [22], the ordinary runs test [23,24], the local reduced chi-square value χ_l^2 and its normal deviate $Z_{\chi_l^2}$.

2.5. Synthetic data generation

Synthetic reference and sample decays were generated by convolution of, respectively, $f_r(t)$ and $f_s(t)$ with the same nonsmoothed measured instrument response function $u(t)$. Several instrument response functions with varying width were used. Each generated d_s, d_r pair had independent Poisson noise. Full details of the decay data simulations are given elsewhere [15]. Simulations, individual and global analysis calculations were performed on an IBM 6150-125 computer in single precision.

3. Results

3.1. Performance of general global analysis

The performance of general global analysis was tested using four simulated decay curves. Four different decay laws were chosen to demonstrate the general applicability of the analysis method. A monoexponential decay with lifetime τ_1 and preexponential α_1 measured against a single exponential reference decay with lifetime τ_r was selected as first decay curve. For this system, the decay may be fitted with three parameters $(\alpha_1, \tau_1, \tau_r; p = 1)$ such that:

$$\tilde{f}_s(t) = \sum_{j=1}^{p} \alpha_j \left[\delta(t) + (1/\tau_r - 1/\tau_j)\exp(-t/\tau_j)\right] \tag{13}$$

For the first curve, all three parameters are 'new' and may be labeled 1–3:

$(\alpha_1, \tau_1, \tau_r)_{\text{curve 1}} = (1,2,3)$ (see table 1A, row 1)

For the second curve, consider a biexponential decay with decay times τ_1 and τ_2 measured against the same single exponential reference with lifetime τ_r (eq. 13, $p = 2$). Let us assume that τ_1 is the same as in the first curve and that τ_2 is identical

to the lifetime of the third curve. τ_r is invariant between the three curves and was kept constant during the fitting procedure. Since there are no linkages between the preexponentials, the five parameters needed to describe the decay may be labeled as:

$$(\alpha_1, \tau_1, \alpha_2, \tau_2, \tau_r)_{\text{curve 2}} = (4,2,5,6,3)$$

(see table 1A, row 2)

As third curve we selected arbitrarily the fluorescence decay of a probe in a micellar system quenched by an immobile quencher. For this system, the fitting function is [25]:

$$\tilde{f}_s(t) = \alpha\{\delta(t) + [1/\tau_r - 1/\tau - A_3 A_4 \exp(-A_4 t)] \times \exp[-t/\tau - A_3(1 - \exp(-A_4 t))]\} \quad (14)$$

For this curve the parameters are labeled as:

$$(\alpha, \tau, A_3, A_4, \tau_r)_{\text{curve 3}} = (7,6,8,9,3)$$

(see table 1A, row 3)

The last curve describes the same phenomenon as the third, but is measured against the instrument response function. The intramicellar quenching rate constant, A_4, is assumed to be invariant between curves 3 and 4. The fitting function appropriate for curve 4 is given by [26,27]:

$$f_s(t) = \alpha \exp\{-A_2 t - S_3[Q][1 - \exp(-A_4 t)]\} \quad (15)$$

For this curve the parameters have the indices:

$$(\alpha, A_2, S_3, A_4)_{\text{curve 4}} = (10,11,12,9)$$

(see table 1A, row 4)

The results of the simultaneous analysis of these four arbitrary curves are listed in table 1B. Global analysis recovered all parameters very accurately with good statistics ($\chi^2_g = 1.028$, $Z_{\chi^2_g} = 0.887$). The parameter estimates from individual analyses are compiled in table 1C. Single-exponential analysis of curve 1 (eq. 13 with $p = 1$) gave – as expected – results that are in excellent agreement with those obtained by multiple-curve analysis. The same was true for the individual analysis of curve 4 according to eq. 15. It has been shown [25] that, when the average number of quenchers per micelle is 0.8 and the number of data points equals $\frac{1}{2}$K, accurate single-curve parameter values are obtained. The parameters of the biexponential model (eq. 15 with $p = 2$) recovered by individual analysis of curve 2 were not that precise. In particular, the short decay time τ_1 with a relatively small contribution (13%) had rather large errors. Individual analysis of curve 3 (eq. 14) also gave large errors compared to multiple-curve analysis. The superior performance of global analysis in the recovery of parameters is evident. Indeed, a short decay time contributing little to the total fluorescence (curve 2) and quenching in micellar systems when the average number of (immobile) quenchers per micelle is low (curve 3, $A_3 = 0.1$) [25] gives rise to decays that are difficult to fit precisely by single-curve analysis (table 1C).

3.2. Global analysis of fluorescence decays of Trp in phosphate buffer at pH 6.0

Fluorescence decays of Trp in phosphate buffer at pH 6.0 (21° C) were collected at emission wavelengths ranging from 310 to 440 nm.

Simultaneous analysis of seven curves measured at 310, 320, 340, 360, 400, 420 and 440 nm against *p*-terphenyl (310–360 nm; $\tau_r = 1.04$ ns, held fixed) and dimethyl-POPOP (400–440 nm; $\tau_r = 1.24$ ns, held fixed) indicated that Trp (pH 6.0 at 21° C) decays biexponentially with decay times $\tau_1 = 760 \pm 11$ ps and $\tau_2 = 2.83 \pm 0.002$ ns ($\chi^2_g = 1.056$, $Z_{\chi^2_g} = 2.341$). The two decay times were invariant (linked) between the decay curves. The preexponentials varied with wavelength: the short decay time τ_1 contributed more to the total fluorescence at shorter analysis wavelengths. A monoexponential model was inadequate to describe the decay data ($\chi^2_g = 6.247$, $Z_{\chi^2_g} = 217.810$). Analysis of the individual curves also confirmed that two and no more than two decay components were necessary to fit Trp decays at pH 6.0 (21° C).

Global analysis of two Trp decays observed at 320 and 360 nm showed that a biexponential model with decay times of 2.60 ± 0.01 ns and 720 ± 20 ps was necessary to describe adequately the decays at 25.6° C ($\chi^2_g = 1.027$, $Z_{\chi^2_g} = 0.601$).

The preexponentials were different at the two emission wavelengths, while the decay times were linked between the curves. Similar global analyses of decays observed at 320, 360 and 400 nm were performed for each individual temperature. The results showed that a biexponential fitting function was necessary to specify the decay data at each temperature (from 25.6 to 55.1° C). The short decay time was independent of temperature, while the long decay time decreased from 2.60 ns at 25.6° C to 1.12 ns at 55.1° C. The recovered long decay times τ_2 could be described by eq. 16:

$$\tau_2^{-1} = k_{ot}^2 + A^2 \exp(-E_a^2/RT) \qquad (16)$$

with $k_{ot}^2 = 1.3 \times 10^8$ s^{-1}, $A^2 = 7.9 \times 10^{13}$ s^{-1} and $E_a^2 = 31.4$ kJ/mol (correlation coefficient 0.999).

3.2.1. Quenching

Fourteen fluorescence decays of Trp in phosphate buffer (pH 6.0) at 22.5° C were collected at 320, 360 and 400 nm in the presence of acrylamide quencher concentrations ranging from 0 to 6×10^{-2} M. *p*-Terphenyl ($\tau_r = 1.04$ ns, held fixed) and xanthione ($\tau_r = 45$ ps, held fixed) were used as standard. The decays were analyzed globally according to eq. 2 with $\tilde{f}_s(t)$ given by eq. 6 ($p = 2$). k_{oq}^1, k_q^1, k_{oq}^2 and k_q^2 were linked between all curves and were freely adjustable. A satisfactory fit ($\chi_g^2 = 1.028$, $Z_{\chi_g^2} = 1.635$) was obtained with $k_{oq}^1 = 1.24 \pm 0.03 \times 10^9$ s^{-1}, $k_q^1 = 9.52 \pm 6.19 \times 10^8$ M^{-1} s^{-1}, $k_{oq}^2 = 3.57 \pm 0.02 \times 10^8$ s^{-1} and $k_q^2 = 4.92 \pm 0.03 \times 10^9$ M^{-1} s^{-1}. The large standard deviation of k_q^1 is noticeable. Analyzing the same data set globally with $k_q^1 = 0$ also gave a good fit ($\chi_g^2 = 1.028$, $Z_{\chi_g^2} = 1.646$) with $k_{oq}^1 = 1.28 \pm 0.01 \times 10^9$ s^{-1}, $k_{oq}^2 = 3.59 \pm 0.01 \times 10^8$ s^{-1} and $k_q^2 = 4.88 \pm 0.02 \times 10^9$ M^{-1} s^{-1}. Global analysis with the two quenching rate constants linked ($k_q^1 = k_q^2$) also gave an acceptable fit but the χ_g^2 ($Z_{\chi_g^2}$) value was somewhat higher ($\chi_g^2 = 1.035$, $Z_{\chi_g^2} = 2.056$). The estimated parameters were $k_{oq}^1 = 1.06 \pm 0.01 \times 10^9$ s^{-1}, $k_{oq}^2 = 3.49 \pm 0.01 \times 10^8$ s^{-1} and $k_q^1 = k_q^2 = 5.08 \pm 0.03 \times 10^9$ M^{-1} s^{-1}. When the decays were analyzed individually (eq. 13, $p = 2$), satisfactory fits were obtained in all cases. The recovered long decay times τ_2 were subsequently analyzed using eq. 17:

$$\tau_2^{-1} = k_{oq}^2 + k_q^2[Q] \qquad (17)$$

yielding $k_{oq}^2 = 3.58 \pm 0.10 \times 10^8$ s^{-1} and $k_q^2 = 4.96 \pm 0.20 \times 10^9$ M^{-1} s^{-1} (correlation coefficient 0.992). The corresponding analysis for the decay times τ_1 had a correlation coefficient of 0.230. The plots of τ_1^{-1} and τ_2^{-1} as a function of [Q] are shown in fig. 1.

3.2.2. Temperature dependence

23 fluorescence decays of Trp in phosphate buffer (pH 6.0) were collected at 320, 360 and 400 nm at temperatures ranging from 25.6 to 60.3° C. *p*-Terphenyl was used as single-exponential standard. The decays were analyzed globally using eq. 2 with $\tilde{f}_s(t)$ given by eq. 8 ($p = 2$). When k_{ot}^1, A^1, E_a^1, k_{ot}^2, A^2 and E_a^2 were linked between all curves and freely adjustable, an adequate fit ($\chi_g^2 = 1.029$, $Z_{\chi_g^2} = 2.197$) was obtained with $k_{ot}^1 = 1.3 \times 10^9$ s^{-1}, $A^1 = 3.5 \times 10^{13}$ s^{-1}, $E_a^1 = 93.3$ kJ/mol,

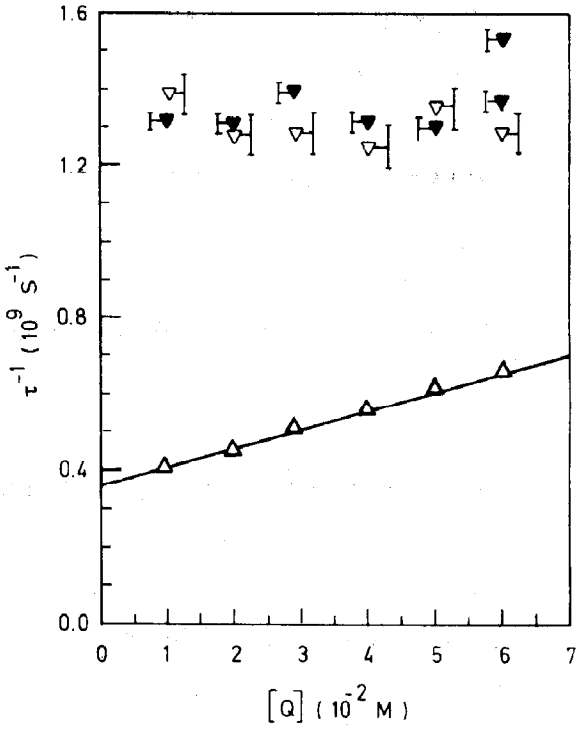

Fig. 1. Reciprocal single-curve decay times of Trp as a function of quencher concentration. Short decay time at (▼) $\lambda_{em} = 320$ nm and at (▽) $\lambda_{em} = 360$ nm, long decay time at (△) $\lambda_{em} = 320$ nm and 360 nm. The error bars represent the standard deviations on the estimated decay times. The standard deviations on the long decay time are within the plotting symbols.

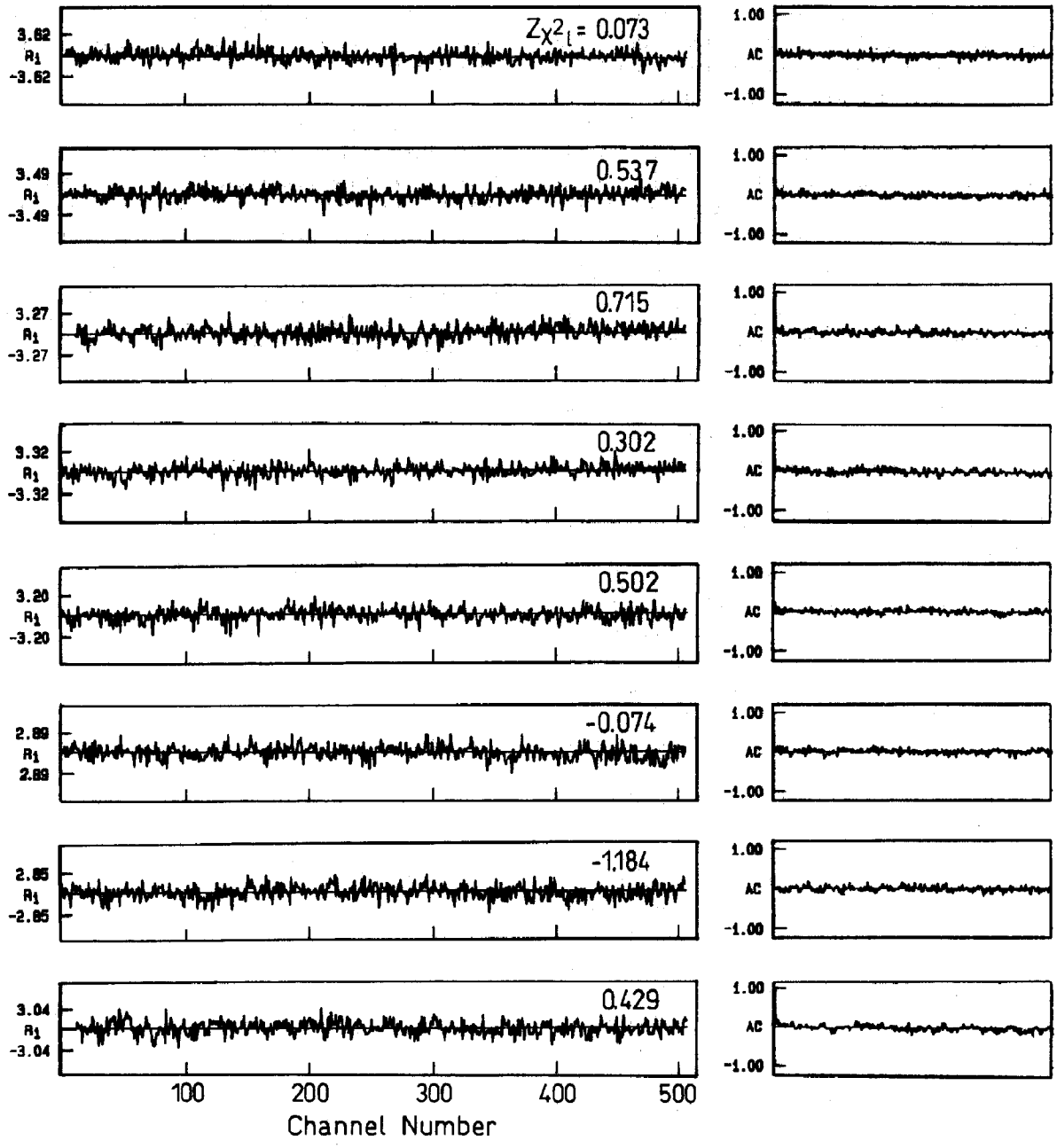

Fig. 2. Weighted residuals (R_i) and autocorrelation functions (AC) of eight Trp decay data fits selected randomly out of 42 analyzed globally under different experimental conditions (analysis wavelength, temperature and quencher concentration). The local $Z_{\chi^2_l}$ statistic is given for each fit (see text and table 2).

$k_{ot}^2 = 4.3 \times 10^7\ s^{-1}$, $A^2 = 8.8 \times 10^{12}\ s^{-1}$ and $E_a^2 = 25.3$ kJ/mol. The activation energy of the fast decay component is enormous. When the activation energies for both decay components were linked ($E_a^1 = E_a^2$), a satisfactory fit ($\chi_g^2 = 1.020$, $Z_{\chi_g^2} = 1.485$) was obtained with $k_{ot}^1 = 1.3 \pm 0.04 \times 10^9\ s^{-1}$, $A^1 = 2.6 \times 10^5 \pm 1.6 \times 10^{12}\ s^{-1}$, $k_{ot}^2 = 9.5 \pm 0.7 \times 10^7\ s^{-1}$, $A^2 = 3.0 \pm 0.5 \times 10^{13}\ s^{-1}$ and $E_a^1 = E_a^2 = 28.7 \pm 0.5$ kJ/mol. The frequency factor of the fast decay component is very small and has an extremely large standard deviation. These two global data analyses indicate that the short decay time τ_1 is independent of temperature. Indeed, the best fit ($\chi_g^2 = 1.019$, $Z_{\chi_g^2} = 1.417$) was obtained when τ_1 was assumed to be independent of temperature while τ_2 was temperature dependent. The recovered decay parameters were: $k_{ot}^1 = 1.3 \pm 0.01 \times 10^9\ s^{-1}$, $k_{ot}^2 = 9.6 \times 10^7\ s^{-1}$, $A^2 = 3.2 \times 10^{13}\ s^{-1}$ and $E_a^2 = 28.9$ kJ/mol. The 23 decays were also analyzed individually as biexponentials (eq. 13, $p = 2$). Valid fits were obtained in all cases. The long decay time values τ_2 were also fitted to eq. 16, yielding the following values: $k_{ot}^2 = 1.3 \times 10^8\ s^{-1}$, $A^2 = 6.1 \times 10^{13}\ s^{-1}$ and $E_a^2 = 30.7$ kJ/mol (correlation coefficient 0.997). The nonlinear analysis of the short decay times did not converge. The 23 Trp decays were also analyzed globally as biexponentials (eq. 13, $p = 2$, *p*-terphenyl as reference with τ_r held fixed) with τ_1 linked between all decays. A perfect global fit ($\chi_g^2 = 0.999$, $Z_{\chi_g^2} = -0.039$) was found with $\tau_1 = 717 \pm 12$ ps, equivalent to $k_{ot}^1 = 1.4 \times 10^9\ s^{-1}$. Describing the long decay times τ_2 by eq. 16 gave $k_{ot}^2 = 5.2 \times 10^7\ s^{-1}$, $A^2 = 1.3 \times 10^{13}\ s^{-1}$ and $E_a^2 = 26.3$ kJ/mol (correlation coefficient 0.997).

3.2.3. *Trp fluorescence decays as functions of temperature, quencher concentration and analysis wavelength*

42 fluorescence decays of Trp in phosphate buffer (pH 6.0) were collected at 310, 320, 340, 360, 400, 420 and 440 nm at temperatures ranging from 25.6 to 60.3°C. *p*-Terphenyl, dimethyl-POPOP and xanthione were used as references. The decays were analyzed globally using eq. 2 with $f_s(t)$ corresponding to three different decay laws:

Table 2

Pictorial representation of global mapping table for the global analysis with 42 experiments and three different decay laws

Boxed decay parameters are linked, while *X* denotes unlinked parameters α^1 and α^2. See text for more details.

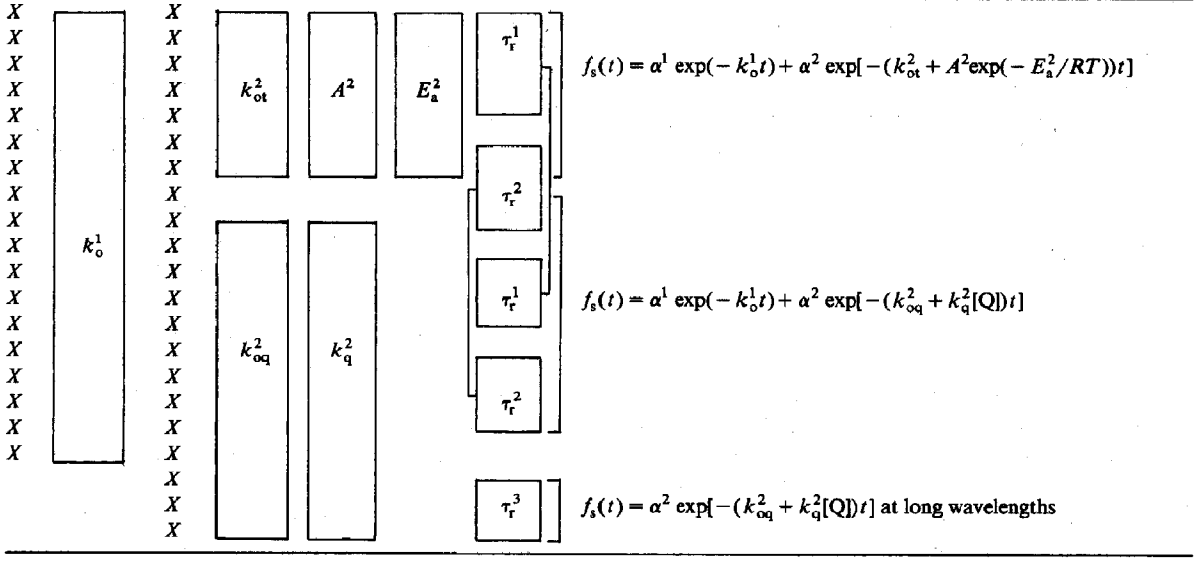

$$f_s(t) = \alpha^1 \exp(-k_o^1 t) + \alpha^2 \exp\left[-\left(k_{ot}^2 + A^2 \exp(-E_a^2/RT)\right)t\right] \quad (18)$$

$$f_s(t) = \alpha^1 \exp(-k_o^1 t) + \alpha^2 \exp\left[-\left(k_{oq}^2 + k_q^2[Q]\right)t\right] \quad (19)$$

$$f_s(t) = \alpha^2 \exp\left[-\left(k_{oq}^2 + k_q^2[Q]\right)t\right] \quad (20)$$

20042 data points were included and 91 free-running parameters had to be estimated in one global analysis. A pictorial view of the global mapping table is given in table 2. The decays as a function of temperature were analyzed according to eq. 18 with k_o^1, k_{ot}^2, A^2 and E_a^2 linked between the curves. The decays as a function of quencher concentration at 22.5 °C were analyzed according to eq. 19 with k_o^1, k_{oq}^2 and k_q^2 linked. At long wavelengths, where only the component with decay time τ_2 contributes, the decays were described by eq. 20 with k_{oq}^2 and k_q^2 linked. The reference lifetimes τ_r^1, τ_r^2 and τ_r^3 were cross-linked. All parameters were adjustable. An excellent fit ($\chi_g^2 = 1.018$, $Z_{\chi_g^2} = 1.813$; fig. 2) was obtained with $k_o^1 = 1.4 \pm 0.01 \times 10^9\ s^{-1}$, $k_{ot}^2 = 1.0 \pm 0.2 \times 10^8\ s^{-1}$, $A^2 = 2.5 \pm 1.1 \times 10^{13}\ s^{-1}$, $E_a^2 = 28.3 \pm 1.2$ kJ/mol, $k_{oq}^2 = 3.6 \pm 0.004 \times 10^8\ s^{-1}$ and $k_q^2 = 4.8 \pm 0.02 \times 10^9\ M^{-1}\ s^{-1}$. The lifetimes of *p*-terphenyl, dimethyl-POPOP and xanthione in isooctane were 1.094 ± 0.009 ns, 1.226 ± 0.004 ns and 45 ± 1 ps, respectively.

The above-mentioned decays of Trp were also analyzed as biexponentials (eq. 13, $p = 2$) with τ_1 invariant between all decays. When the reference lifetimes were fixed at their known values an adequate fit was obtained ($\chi_g^2 = 1.003$, $Z_{\chi_g^2} = 0.340$). The lifetime τ_1 was found to be 753 ± 7 ps.

4. Discussion

The results obtained for simulated and real decay data sets clearly demonstrate the power of the general global analysis. The global results obtained for synthetic decays show that all model parameters are recovered very accurately (table 1B). Curves 2 and 3, which are difficult to fit by single-curve analysis (table 1C), are fitted very precisely by simultaneous analysis. As exemplified by the complicated fitting schemes (e.g., see table 2) for Trp decays, the general simultaneous analysis allows the evaluation of complex competing models. Because of its potential to make intricate linking between parameters that are common between related curves and/or within one curve, we expect that general global analyses will supersede analyses in which only lifetimes can be linked.

Tryptophan has been extensively used as an intrinsic fluorescent probe in investigations of protein structure and dynamics. A detailed understanding of the photophysics of tryptophan is imperative for a proper interpretation of the experimental results (for reviews of photophysical studies on Trp, see refs. 28 and 29). Evidence obtained by numerous workers [30–36] clearly shows that Trp fluorescence decays at pH ≤ 7 are biexponential with a subnanosecond component. Our global analyses of multiple Trp fluorescence decay curves at pH 6.0 as a function of temperature, added solute quencher and emission wavelength confirm the single-curve analysis results. The possibility of a time-dependent intramolecular quenching process such as that suggested by Robbins et al. [33] can be ruled out. Above pH 7, the decays become triple-exponential with the long component due to anionic Trp [34,37]. The most generally accepted model to explain the photophysics of zwitterionic Trp is the rotamer model, originally proposed by Wahl and co-workers [38] for tryptophan diketopiperazines. It postulates that different rotamers about the C_α–C_β dihedral angle (χ_1) which do not interconvert on the fluorescence time scale are responsible for the different decay times. Using molecular dynamics simulations, a new model has been proposed [39] for Trp biexponential fluorescence decays in terms of two χ_2 rotamers (about the C_β–C_γ dihedral) each consisting of equilibrated (on the fluorescence time scale) distributions of χ_2 conformers. Proton transfer from the α-ammonium group to the excited indole ring [32,33,40,41] and/or electron transfer from the excited indole ring to various electrophiles [35,36] have been suggested as mechanisms for intramolecular quenching of singlet excited Trp in aqueous solution. Using single-curve decay time

estimates as a function of temperature, Chang et al. [35] showed that the two decay times had nearly identical activation energies but different prefactors. This is consistent with an electron-transfer process giving both decay times, since the activation energy depends on the identity of the donor-acceptor pair which is the same in the different conformers, whereas the frequency factor depends on orientation. The temperature-dependent decay time data obtained by simultaneous analysis of multiple tryptophan fluorescence decays at pH 6.0 are in contrast with their results. Indeed, we found that the short decay time τ_1 is independent of temperature, while the long decay time τ_2 has an activation energy of about 28 kJ/mol with a prefactor of 3×10^{13} s^{-1}. However, based on these data only, it would be premature to rule out electron transfer as a possible mechanism for the nonradiative decay of zwitterionic Trp. In order to understand fully the photophysics of tryptophan more investigations are needed. Our preliminary data on Trp photophysics unquestionably demonstrate the power of global analysis in exploring complex photophysical behavior.

Appendix: Recursion formulas for the global estimation of decay rate constants, activation energies and frequency factors

When $f_s(t)$ is a sum of exponentials (eq. A1),

$$f_s(t) = \sum_{m=1}^{p} \alpha^m \exp\left(-t\sum k^m\right) \tag{A1}$$

the numerical formulas for the calculation of the sample fluorescence response, $d_s(t)^c$, and its partial derivatives with respect to the parameters can be simplified. The convolution integral can be written as

$$d_s(t)^c = \int_0^t u(s)^o \left\{ \sum_{m=1}^{p} \alpha^m \exp\left[-(t-s)\sum k^m\right] \right\} ds \tag{A2}$$

where $u(s)^o$ denotes the observed (measured) instrument response function at time s, and $d_s(t)^c$ the calculated fluorescence response at time t. Eq. A2 can be written as

$$d_s(t)^c = \sum_{m=1}^{p} \int_0^t \alpha^m u(s)^o \exp\left[-(t-s)\sum k^m\right] ds \tag{A3}$$

In single-photon timing experiments, the fluorescence decay curves are collected in discrete channels. Let us write $d_{s,i}$ and u_i for $d_s(t_i)^c$ and $u(t_i)^o$, respectively, and denote by ϵ the time duration of one channel of the multichannel analyzer. Eq. A3 may then be written as

$$d_{s,i} = \sum_{m=1}^{p} d_{s,i}^m \tag{A4}$$

$d_{s,i}^m$ is the calculated sample fluorescence response in the i-th channel due to the m-th exponential component. Using the trapezoidal rule to compute the convolution integral, one has

$$d_{s,i}^m = \epsilon \left\{ 0.5\alpha^m u_0 \exp\left(-\epsilon i \sum k^m\right) + \sum_{j=1}^{i-1} \alpha^m u_j \exp\left[-\epsilon(i-j)\sum k^m\right] + 0.5\alpha^m u_i \right\} \tag{A5}$$

$$d_{s,i+1}^m = \epsilon \left\{ 0.5\alpha^m u_0 \exp\left[-\epsilon(i+1)\sum k^m\right] + \sum_{j=1}^{i-1} \alpha^m u_j \exp\left[-\epsilon(i+1-j)\sum k^m\right] + \alpha^m u_i \exp\left(-\epsilon\sum k^m\right) + 0.5\alpha^m u_{i+1} \right\} \tag{A6}$$

Hence

$$d_{s,i+1}^m = \left(d_{s,i}^m + 0.5\epsilon\alpha^m u_i\right) \times \exp\left(-\epsilon\sum k^m\right) + 0.5\epsilon\alpha^m u_{i+1} \tag{A7}$$

and

$$\partial d^m_{s,i}/\partial \alpha^m = d^m_{s,i}/\alpha^m \tag{A8}$$

Let us now consider the quenching and temperature dependence.

A1. Quenching: $\Sigma k^m = k^m_{oq} + k^m_q$ *[Q]*

The partial derivatives of $d^m_{s,i+1}$ with respect to k^m_{oq} and k^m_q are

$$\frac{\partial d^m_{s,i+1}}{\partial k^m_{oq}} = \left[\frac{\partial d^m_{s,i}}{\partial k^m_{oq}} - \epsilon\left(d^m_{s,i} + 0.5\epsilon\alpha^m u_i\right)\right] \times \exp\left(-\epsilon\sum k^m\right) \tag{A9}$$

$$\frac{\partial d^m_{s,i+1}}{\partial k^m_q} = \left[\frac{\partial d^m_{s,i}}{\partial k^m_q} - \epsilon[\mathrm{Q}]\left(d^m_{s,i} + 0.5\epsilon\alpha^m u_i\right)\right] \times \exp\left(-\epsilon\sum k^m\right) \tag{A10}$$

For Newton-type algorithms, second partial derivatives are required.

$$\frac{\partial^2 d^m_{s,i}}{\partial \alpha^2} = 0 \tag{A11}$$

$$\frac{\partial^2 d^m_{s,i}}{\partial \alpha^m \partial k^m_{oq}} = \frac{\partial d^m_{s,i}}{\alpha^m \partial k^m_{oq}} \tag{A12}$$

$$\frac{\partial^2 d^m_{s,i}}{\partial \alpha^m \partial k^m_q} = \frac{\partial d^m_{s,i}}{\alpha^m \partial k^m_q} \tag{A13}$$

$$\frac{\partial^2 d^m_{s,i+1}}{\partial k^{m2}_{oq}} = \left[\frac{\partial^2 d^m_{s,i}}{\partial k^{m2}_{oq}} - \epsilon\left[2\frac{\partial d^m_{s,i}}{\partial k^m_{oq}} - \epsilon\left(d^m_{s,i} + 0.5\epsilon\alpha^m u_i\right)\right]\right] \times \exp\left(-\epsilon\sum k^m\right) \tag{A14}$$

$$\frac{\partial^2 d^m_{s,i+1}}{\partial k^{m2}_q} = \left[\frac{\partial^2 d^m_{s,i}}{\partial k^{m2}_q} - \epsilon[\mathrm{Q}]\left[2\frac{\partial d^m_{s,i}}{\partial k^m_q} - \epsilon[\mathrm{Q}] \times \left(d^m_{s,i} + 0.5\epsilon\alpha^m u_i\right)\right]\right] \exp\left(-\epsilon\sum k^m\right) \tag{A15}$$

$$\frac{\partial^2 d^m_{s,i+1}}{\partial k^m_{oq}\partial k^m_q} = \left[\frac{\partial^2 d^m_{s,i}}{\partial k^m_{oq}\partial k^m_q} - \epsilon\left[\frac{\partial d^m_{s,i}}{\partial k^m_q} + [\mathrm{Q}]\left(\frac{\partial d^m_{s,i}}{\partial k^m_{oq}} - \epsilon\left(d^m_{s,i} + 0.5\epsilon\alpha^m u_i\right)\right)\right]\right] \times \exp\left(-\epsilon\sum k^m\right) \tag{A16}$$

$\partial d^m_{s,i}/\partial \psi^k \neq 0$ only if $m = k$ where ψ^k is a fitting parameter of the k-th exponential component. $\partial^2 d^m_{s,i}/\partial \psi^k \partial \phi^j \neq 0$ only if $m = k = j$ (ψ^k and ϕ^j: fitting parameters of the k-th and j-th exponential component, respectively) and if ψ^k and ϕ^j are not both preexponential factors.

A2. Temperature dependence: $\Sigma k^m = k^m_{ot} + A^m \exp(-E^m_a/RT)$

The partial derivatives of $d^m_{s,i}$ with respect to α^m and k^m_{ot} are given by eqs. A8 and A9 with $\Sigma k^m = k^m_{ot} + A^m \exp(-E^m_a/RT)$.

$$\frac{\partial d^m_{s,i+1}}{\partial A^m} = \left[\frac{\partial d^m_{s,i}}{\partial A^m} - \epsilon \exp(-E^m_a/RT) \times \left(d^m_{s,i} + 0.5\epsilon\alpha^m u_i\right)\right] \exp\left(-\epsilon\sum k^m\right) \tag{A17}$$

$$\frac{\partial d^m_{s,i+1}}{\partial E^m_a} = \left[\frac{\partial d^m_{s,i}}{\epsilon E^m_a} + \frac{\epsilon A^m}{RT}\exp(-E^m_a/RT) \times \left(d^m_{s,i} + 0.5\epsilon\alpha^m u_i\right)\right] \exp\left(-\epsilon\sum k^m\right) \tag{A18}$$

Second partial derivatives are obtained in analogy with the derivatives, eqs. A11–A16.

For reference convolution, the calculated sample fluorescence response $d_s(t)^c$ is given by

$$d_s(t)^c = \sum_{m=1}^{p} \alpha^m d_r(t)^o + \sum_{m=1}^{p} g^m(t)^c \tag{A19}$$

with

$$g^m(t)^c = \int_0^t \alpha^m \left(1/\tau_r - \sum k^m\right) d_r(s)^o \times \exp\left[-(t-s)\sum k^m\right] \mathrm{d}s \tag{A20}$$

where τ_r denotes the reference lifetime, and $d_r(t)^o$

the observed (experimental) reference decay at time t. In the algorithm the discrete form of eq. A19 is used. Let us denote by $d_{r,i}$ and g_i^m the values of $d_r(t)^o$ and $g^m(t)^c$ in the i-th channel. Eq. A19 may then be written as

$$d_{s,i} = \sum_{m=1}^{p} \alpha^m d_{r,i} + \sum_{m=1}^{p} g_i^m \tag{A21}$$

In analogy with the recursion formulas derived above the following expressions can be used to reduce computing time

$$g_{i+1}^m = \left[g_i^m + 0.5\epsilon\alpha^m \left(1/\tau_r - \sum k^m\right) d_{r,i} \right] \times \exp\left(-\epsilon \sum k^m\right) + 0.5\epsilon\alpha^m \left(1/\tau_r - \sum k^m\right) d_{r,i+1} \tag{A22}$$

$$\partial g_i^m / \partial \alpha^m = g_i^m / \alpha^m \tag{A23}$$

$$\frac{\partial g_{i+1}^m}{\partial \tau_r} = \exp\left(-\epsilon \sum k^m\right) \left[\frac{\partial g_i^m}{\partial \tau_r} - \frac{0.5\epsilon\alpha^m d_{r,i}}{\tau_r^2} \right] - \frac{0.5\epsilon\alpha^m d_{r,i+1}}{\tau_r^2} \tag{A24}$$

Let us consider the quenching and temperature dependence.

A3. Quenching: $\sum k^m = k_{oq}^m + k_q^m [Q]$

The partial derivatives of g_{i+1}^m with respect to k_{oq}^m and k_q^m are

$$\frac{\partial g_{i+1}^m}{\partial k_{oq}^m} = \left[\frac{\partial g_i^m}{\partial k_{oq}^m} - \epsilon \left(g_i^m + 0.5\epsilon\alpha^m d_{r,i} \times \left(1/\tau_r + 1/\epsilon - \sum k^m\right)\right) \right] \times \exp\left(-\epsilon \sum k^m\right) - 0.5\epsilon\alpha^m d_{r,i+1} \tag{A25}$$

$$\frac{\partial g_{i+1}^m}{\partial k_q^m} = \left[\frac{\partial g_i^m}{\partial k_q^m} - \epsilon [Q] \left(g_i^m + 0.5\epsilon\alpha^m d_{r,i} \times \left(1/\tau_r + 1/\epsilon - \sum k^m\right)\right) \right] \times \exp\left(-\epsilon \sum k^m\right) - 0.5\epsilon [Q] \alpha^m d_{r,i+1} \tag{A26}$$

A4. Temperature dependence: $\sum k^m = k_{ot}^m + A^m \exp(-E_a^m/RT)$

The partial derivatives of g_i^m with respect to α^m, τ_r and k_{ot}^m are given by eqs. A23–A25 with $\sum k^m = k_{ot}^m + A^m \exp(-E_a^m/RT)$.

$$\frac{\partial g_{i+1}^m}{\partial A^m} = \left[\frac{\partial g_i^m}{\partial A^m} - \epsilon \exp\left(-E_a^m/RT\right) \times \left(g_i^m + 0.5\epsilon\alpha^m d_{r,i} \left(1/\tau_r + 1/\epsilon - \sum k^m\right)\right) \right] \times \exp\left(-\epsilon \sum k^m\right) - 0.5\epsilon\alpha^m \times \exp\left(-E_a^m/RT\right) d_{r,i+1} \tag{A27}$$

$$\frac{\partial g_{i+1}^m}{\partial E_a^m} = \left[\frac{\partial g_i^m}{\partial E_a^m} + \frac{\epsilon A^m}{RT} \exp\left(-E_a^m/RT\right) \times \left(g_i^m + 0.5\epsilon\alpha^m d_{r,i} \left(1/\tau_r + 1/\epsilon - \sum k^m\right)\right) \right] \times \exp\left(-\epsilon \sum k^m\right) + 0.5\epsilon\alpha^m A^m \times \exp\left(-E_a^m/RT\right) d_{r,i+1}/RT \tag{A28}$$

Acknowledgements

N.B. is a 'Bevoegdverklaard Navorser' of the 'Fonds voor Geneeskundig Wetenschappelijk Onderzoek' (FGWO, Belgium). L.D.J. thanks the 'Instituut ter aanmoediging van het Wetenschappelijk Onderzoek in de Nijverheid en de Landbouw' (IWONL, Belgium) for a predoctoral fellowship. This research was supported in part by FGWO grant no. 3.0099.86.

References

1 J.N. Demas, Excited state lifetime measurements (Academic Press, New York, 1983).
2 R.B. Cundall and R.E. Dale, Life Sci. 69 (1983).
3 D.V. O'Connor and D. Phillips, Time-correlated single photon counting (Academic Press, London, 1984).

4 J. Eisenfeld and C.C. Ford, Biophys. J. 26 (1979) 73.
5 J.R. Knutson, J.M. Beechem and L. Brand, Chem. Phys. Lett. 102 (1983) 501.
6 M. Ameloot, J.M. Beechem and L. Brand, Biophys. Chem. 23 (1986) 155.
7 J.M. Beechem, M. Ameloot and L. Brand, Life Sci. (1989) in the press.
8 N. Boens, M. Van den Zegel and F.C. De Schryver, Chem. Phys. Lett. 111 (1984) 340.
9 R.M.C. Dawson, D.C. Elliott, W.H. Elliott and K.M. Jones, Data for biochemical research, 2nd edn. (Oxford University Press, New York, 1969) p. 489.
10 N. Boens, M. Van den Zegel, F.C. De Schryver and G. Desie, in: From photophysics to photobiology, eds. A. Favre, R. Tyrrell and J. Cadet (Elsevier, Amsterdam, 1987) p. 93.
11 P. Gauduchon and P. Wahl, Biophys. Chem. 8 (1978) 87.
12 R.W. Wijnaendts van Resandt, R.H. Vogel and S.W. Provencher, Rev. Sci. Instrum. 53 (1982) 1392.
13 L.J. Libertini and E.W. Small, Anal. Biochem. 138 (1984) 314.
14 M. Zuker, A.G. Szabo, L. Bramall, D.T. Krajcarski and B. Selinger, Rev. Sci. Instrum. 56 (1985) 14.
15 M. Van den Zegel, N. Boens, D. Daems and F.C. De Schryver, Chem. Phys. 101 (1986) 311.
16 N. Boens, M. Ameloot, I. Yamazaki and F.C. De Schryver, Chem. Phys. 121 (1988) 73.
17 A.E. McKinnon, A.G. Szabo and D.R. Miller, J. Phys. Chem. 81 (1977) 1564.
18 D.V. O'Connor, W.R. Ware and J.C. Andre, J. Phys. Chem. 83 (1979) 1333.
19 R.I. Jennrich and M.L. Ralston, Annu. Rev. Biophys. Bioeng. 8 (1979) 195.
20 D.W. Marquardt, J. Soc. Ind. Appl. Math. 11 (1963) 431.
21 A. Grinvald and I.Z. Steinberg, Anal. Biochem. 59 (1974) 583.
22 J. Durbin and G.S. Watson, Biometrika 37 (1950) 409; 38 (1951) 159; 58 (1971) 1.
23 R.F. Gunst and R.L. Mason, Regression analysis and its application, a data-oriented approach (Dekker, New York, 1980).
24 N.R. Draper and H. Smith, Applied regression analysis, 2nd edn. (Wiley, New York, 1981).
25 N. Boens, A. Malliaris, M. Van der Auweraer, H. Luo and F.C. De Schryver, Chem. Phys. 121 (1988) 199.
26 P. Infelta, M. Grätzel and J.K. Thomas, J. Phys. Chem. 78 (1974) 190.
27 M. Tachiya, Chem. Phys. Lett. 33 (1975) 289.
28 D. Creed, Photochem. Photobiol. 39 (1984) 537.
29 J.M. Beechem and L. Brand, Annu. Rev. Biochem. 54 (1985) 43.
30 D.M. Rayner and A.G. Szabo, Can. J. Chem. 56 (1978) 743.
31 A.G. Szabo and D.M. Rayner, J. Am. Chem. Soc. 102 (1980) 554.
32 G.S. Beddard, G.R. Fleming, G. Porter and R.J. Robbins, Phil. Trans. R. Soc. Lond. A298 (1980) 321.
33 R.J. Robbins, G.R. Fleming, G.S. Beddard, G.W. Robinson, P.J. Thistlethwaite and G.J. Woolfe, J. Am. Chem. Soc. 102 (1980) 6271.
34 E. Gudgin, R. Lopez-Delgado and W.R. Ware, Can. J. Chem. 59 (1981) 1037.
35 M.C. Chang, J.W. Petrich, D.B. McDonald and G.R. Fleming, J. Am. Chem. Soc. 105 (1983) 3819.
36 J.W. Petrich, M.C. Chang, D.B. McDonald and G.R. Fleming, J. Am. Chem. Soc. 105 (1983) 3824.
37 J.-E. Löfroth, Eur. Biophys. J. 13 (1985) 45.
38 B. Donzel, P. Gauduchon and P. Wahl, J. Am. Chem. Soc. 96 (1974) 801.
39 R.A. Engh, L.X.-Q. Chen and G.R. Fleming, Chem. Phys. Lett. 126 (1986) 365.
40 I. Saito, H. Sugiyama, A. Yamamoto, S. Muramatsu and T. Matsuura, J. Am. Chem. Soc. 106 (1984) 4286.
41 H. Shizuka, M. Serizawa, T. Shimo, I. Saito and T. Matsuura, J. Am. Chem. Soc. 110 (1988) 1930.